Yield Envelopes for Oblique Pipeline/Soil Interaction in Cohesive Soil using ALE Procedure

Seo, D., Kenny, S. & Hawlader, B.
Faculty of Engineering and Applied Science - Memorial University of Newfoundland, St. John's, NL, Canada
Phillips, R.
C-CORE, St. John's, NL, Canada

ABSTRACT
This study examines the yield envelopes for axial-lateral oblique pipeline/soil interaction in cohesive soil with particular attention to the pipe oblique angle and the pipe burial depth ratio on the basis of LS-DYNA/Explicit ALE formulation. Based on this approach, the soil failure mechanisms were examined as a function of pipe oblique angle. This paper also presents a fact that the yield envelopes should be determined by considering soil failure mechanisms, which is varied with pipe oblique angle: (a) lateral resistance, (b) lateral-axial transition, and (c) axial resistance zones.

RÉSUMÉ
Cette étude examine les enveloppes de rendement des pipelines oblique axial-latérale de l'interaction sol / dans des sols cohérents avec une attention particulière à l'angle de tube oblique et le rapport profondeur du tuyau d'inhumation sur la base de LS-DYNA/Explicit ALE formulation. Sur la base de cette approche, les mécanismes de rupture du sol ont été examinés en fonction de l'angle de tube oblique. Cet article présente également un fait que les enveloppes de rendement devraient être déterminés en tenant compte des mécanismes de rupture du sol, qui est varié avec un angle de tube oblique: (a) la résistance latérale, (b) transition latérale-axial, et (c) zones résistance axiale.

1 INTRODUCTION

Pipeline transportation systems deliver hydrocarbon products from field development areas to market over hundreds of kilometers. The pipeline systems may be subject to long-term large deformation geohazards including subsidence, slope movement, frost heave and thaw settlement. The ground displacement field imposes geotechnical loads on the buried pipeline system. This may initiate pipeline deformations, such as ovalization, that affect operations and serviceability conditions. This may also trigger pipeline deformations affecting ultimate limit states with respect to mechanical integrity (e.g., local buckling) and pressure containment (e.g., rupture). The consequences may have significant impact on society, environment, and operations; particularly for service interruption of gas transmission lines.

As proposed in the guidelines such as ALA (2001) and PRCI (Honegger and Nyman 2004, Honegger et al., 2010), numerical simulation of pipeline/soil interaction problems has been generally based on the Winkler-type structural beam-spring model. The soil response is idealized by discrete, nonlinear soil springs representing geotechnical loads acting on the pipeline along three orthogonal axes. The validity of the Winkler-type model to adequately represent realistic soil behaviour and complex, large deformation pipeline/soil interaction events has been questioned (Konuk et al., 2006; Kenny et al., 2007; Bruschi et al., 2010). A significant idealization in the Winkler-type model is the decoupling of orthogonal soil springs where the effects of shear load transfer between adjacent soil springs is ignored. Nevertheless, there is a need for structural modeling procedures to conduct engineering assessments and provide input to informed decision making. For example, structural models can be used to assess pipeline routing, conduct hazard assessment, and assist operational monitoring programs. In recognition of this, there have been recently notable studies to improve yield envelopes for axial-lateral or lateral-vertical oblique pipeline/soil interaction event, by taking into account the coupling effect experimentally or numerically (Phillips et al., 2004; Yimsiri et al., 2004; Guo, 2005; Hsu et al., 2006, Cocchetti et al., 2009; Daiyan et al., 2009, 2010; Pike and Kenny, 2011). From the numerical point of view, special attention is being given to resolve nonlinear large relative pipeline/soil displacement and complex failure mechanisms, by considering the progressive mobilization of soil strength with plastic strain using the Arbitrary Lagrangian Eulerian or Coupled Eulerian Lagrangian formulation implemented in ABABQUS/Explicit. With respect to the CEL method, there are latest research works on free-field ice gouge or coupled ice keel/seabed/pipeline interaction events (Jukes et al., 2008; Phillips et al., 2010; Banneyake et al., 2011; Lele et al., 2011; Pike et al., 2011). On the other hand, there have been a number of studies using the ALE method implemented in LS-DYNA/Explicit Arbiturary Lagrangian Eulerian (Konuk and Gracie. 2004; Konuk and Yu, 2007; Fredj et al., 2008; Fredj and Dinovitzer, .2010) on the focus of ice gouge simulations, upheaval and lateral buckling problems, and permanent ground deformation events. In spite of numerous efforts in the public domain, there is still a lack of technical or engineering evidences for axial, lateral, vertical, and oblique pipeline/soil interaction event, which is absolutely required to establish enhanced structural model for ice keel/soil/pipeline interaction events.

In this study, three-dimensional continuum finite element modelling procedures using LS-DYNA/Explicit ALE examine soil load coupling effects during axial-lateral oblique pipeline/soil interaction events (Fig.1) in cohesive soil. The significance of a variation in the oblique attack angle and burial depth on the yield envelopes is investigated. The soil failure mechanisms are also examined. Based on the simulation results, implications on pipeline engineering design of oblique pipeline/soil interaction event are discussed.

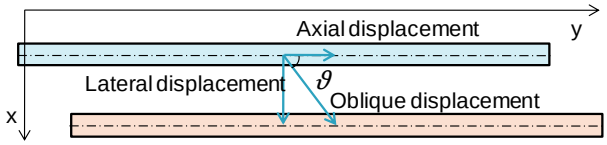

Figure 1. Sketch of pipeline oblique angle

2 NUMERICAL METHOD

2.1 LS-DYNA/Explicit ALE Method

For the simulation of large deformation and large strain mechanisms, Arbitrary Lagrangian Eulerian (ALE) method integrates the beneficial characteristics of Lagrangian and Eulerian formulations to overcome problems associated with numerical instability and solution degradation. Donea et al. (2004) provides a good overview of ALE methods.

The ALE technique can be characterized by three general steps that include:

- standard nonlinear, finite element analysis using explicit techniques within updated Lagrangian formulation for large deformations and large strains,
- remapping of the finite element mesh based on smoothing criteria related to the mesh topology, stress state or strain distribution of the preceding time step, and
- advection phase based on Eulerian formulation where the laws of conservation and momentum are used.

A good advection scheme should be monotonic, conservative and as little dispersive and dissipative as possible. In general, a second order accurate monotonic advection algorithm (e.g. van Leer scheme) is superior to a first order accurate monotonic advection algorithm (e.g. donor cell scheme). In this study, a set of preliminary investigations did not exhibit any significant difference in the pipe-soil interaction simulaitons.

Accurately defining the material interface position requires a tracking algorithm where the Young's method was used. During material transport or advection, the material was described by the volume fraction (VOF) of fluid material in the element. The volume of fraction (VOF) in LS-DYNA/ALE is similar to the Eulerian volume fraction (EVF) in ABAQUS/CEL method. A volume fraction initialisation algorithm (LSTC, 2010) for fluid/structure interaction problems has been implemented into LS-DYNA code and enables accurate modelling of multi-material ALE (MMALE) meshes especially with oil and gas in the pipeline embedded in trench or multiple soil layers.

LS-DYNA uses a modification of the central difference integration method and for explicit schemes the equation of motion is evaluated at the previous time step. The characteristic element length and wave propagation velocity determined the critical time step used in the analysis.

2.2 Fluid-Structure Interaction

For fluid-structure interaction (FSI) problems in LS-DYNA, the fluid interface nodes are considered as the slave and structure interface nodes as the master. The first constraint based method (or kinematic contact) does not conserve total energy and is seldom used, whereas the second penalty based method (or penalty contact) conserves total energy and is the current method of choice. Penalty coupling behaves like a spring system on the intersections (coupling points; NQUAD) and penalty forces are calculated proportionally to the penetration depth (d) and spring stiffness (k):

$$F = k \cdot d \qquad [1]$$

where, k is given in terms of the bulk modulus (K) of the fluid material, the volume (V) of the fluid element and the average area (A) of the fluid segment:

$$k = p_f \frac{KA^2}{V} \qquad [2]$$

where p_f (PFAC) is a penalty factor and its default value (0.1) is used in this study to avoid numerical instability. For high velocity impact events, to prevent issues regarding fluid leakage through the structure, the penalty force (F) in LS-DYNA (LSTC 2006) is bounded by the contact force between two spheres as:

$$F \le \frac{M_s M_m (v_s - v_m)}{\Delta t (M_s + M_m)} \qquad [3]$$

where M_s is the mass of slave or structure, M_m is the mass of master or fluid, (v_s-v_m) is the relative velocity and Δt is the current time step. On the same time, LS-DYNA provides the option (PFAC=load curve) to utilize nonlinear or piecewise linear spring system with penetration dependent stiffness for some problems involving highly compressible gas, such as airbag simulations.

$$F = k(\ )d \qquad [4]$$

The penalty force corresponds to the contact pressure where the frictional force (F_f) is defined by coefficient of friction (μ; FRIC) in Eq.[5]

$$F_f = \mu \cdot F = \mu \cdot k \cdot d \qquad [5]$$

Recently LS-DYNA R5.1 implemented a piecewise nonlinear frictional curve, expressed by Eq.[6], which enables to introduce the Coulomb friction model with the shear stress limit.

$$F_f = \mu(\ )F = \mu(\ )k \cdot d \quad or \quad \mu(\ )k(\ )d \qquad [6]$$

In this study, minimum volume fraction of the fluid in a multi-material ALE element to activate FSI coupling was set to 30% to prevent leakage. Negative volume errors can be encountered at the coupling interface between the Lagrangian (e.g. pipeline) and Eulerian (e.g. soil) interfaces. The main issues are related to the number of quadrature points defining the Lagrangian/Eulerian coupling surface, mesh topology and minimum time step used in the simulation.

For large deformation pipeline/soil interaction events, the interface behaviour, contact mechanics and strain localization requires further investigation and physical data for the calibration and validation of the numerical procedures. This study demonstrates agreement with available data but further investigations will be required to improve the simulation tool and establish confidence in the analysis.

2.3 Material Model

LS-DYNA allows users to simulate a whole range of engineering materials using a variety of over 270 constitutive models. Soil constitutive models as follows are implemented and validated in LS-DYNA/Explicit ALE simulation: (1) von Mises constitutive model (*Mat_003; used in this study), (2) soil and foam model (*Mat_005; Fredj et al., 2008; Fredj and Dinovitzer 2010), (3) piecewise linear plasticity model (*Mat_024) and (4) geological cap model (*Mat_025; Konuk and Gracie; 2004, Konuk and Yu 2007).

The soil and foam model is composed of two independent non-intersecting surfaces that includes a pressure dependent shear failure surface and compaction (pressure-volume strain) surface. By calibrating this model to triaxial compression test data, this model can be related to the Drucker-Prager model. The drawbacks for this model include rather crude tension limiting ability, a lack of associated flow plasticity and no third invariant dependence.

The geologic cap model has two intersecting surface plasticity models, which allows for unloading, stress path dependency and dilatancy. In view of high permeability of cohesionless soil and the dependency of stress-strain response on confining stress, the Drucker-Prager model in *Mat_005 and *Mat_025 is sufficient as a material model for granular soil. To properly characterize the corresponding optimal soil parameters of both models, a series of triaxial compression and hydrostatic compression tests with depth are required. For cohesive soil, consolidated-undrained and consolidated-drained triaxial tests are needed to conduct effective stress analysis.

In this study, a total stress analysis for undrained loading of cohesive soil was conducted using the von Mises yield criterion. Improvements to the soil constitutive model may be required to capture hardening and softening response, rate effects and interface behaviour.

3 OBLIQUE PIPELINE/SOIL INTERACTION MODEL

For axial-lateral oblique pipeline/soil interaction simulations, the 3D continuum finite element model was developed using LS-DYNA/Explicit (Ver. 971 R5.1) multi-material ALE formulation. As depicted in Fig. 2, the model domain is taken to be large enough to eliminate the boundary effects. The continuum model obtained from mesh sensitivity study includes the void, the Eulerian soil, the Lagrangian rigid pipeline, and the void in the pipeline. The void elements are material-free (void) at the initial state of the simulation to consider the upheaval and subsidence of soil surface. The void in the pipeline is modelled using the initial volume-filling command in LS-DYNA to replicate the material-free state in the pipeline.

In LS-DYNA, the only available ALE multi-material element is the eight node constant stress elements with one point integration. This element is used for the Eulerian soil and the void. In this paper, a cohesive soil with a total unit weight of 17.5 kN/m^3 and undrained shear strength of 45 kPa is considered as the Eulerian soil. The pipe with a diameter of D = 95 cm and a thickness of D/t = 30 is discretized as a rigid body such that the pipe does not experience any deformation or ovalisation during axial-lateral movement. The Euler-Lagrange coupling algorithm introduced in this paper is penalty coupling (pipeline/soil friction angle = 25^o) because this method is mainly based on force equilibrium and energy conservation.

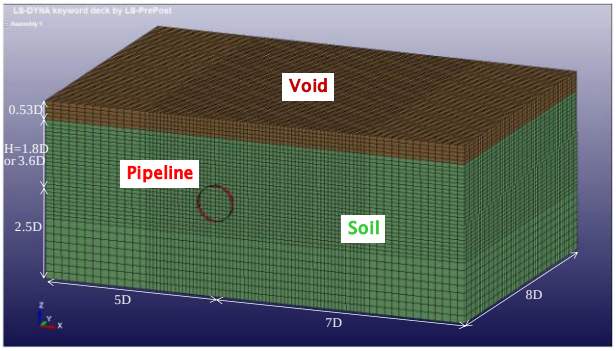

Figure 2. LS-DYNA/Explicit ALE FE model configuration

The simulation is conducted using two steps: (1) geostatic step in which a gravitational acceleration is applied and satisfactory time to reach initial stationary stress state is allowed; (2) Second step in which the pipeline motion in the axial-lateral oblique direction is applied. The aim in this simulation is to investigate the effects of the oblique attack angle (ϑ = 0^o to 90^o) and burial depth (H/D = 1.8 and 3.6; H is the pipe burial depth to pipe centreline or springline) on the yield envelopes.

4 SIMULATION RESULTS AND DISCUSSIONS

4.1 Lateral/Axial Pipeline/Soil Interaction

According to current practical guidelines, the peak lateral and axial soil loads per unit length of pipe in cohesive soil are obtained by:

$$P_u = N_{ch} \cdot c_u \cdot D \quad [7]$$

$$T_u = \pi \cdot D \cdot \alpha \cdot c_u \quad [8]$$

where N_{ch} is lateral bearing capacity factor for cohesive soil and can be derived from the database of

various research works (Hansen 1961, ALA 2001, Honegger and Nyman 2004, Phillips et al., 2004) with the pipe springline depth to pipe diameter ratio. The adhesion factor (α) is a decreasing function of the undrained shear strength. To examine the effect of the ultimate load definition, the ultimate load was estimated using three methods: (1) the load value at the point of intersection of the two straight line portions of the load-displacement curve, (2) the load value at which the curve passes into a steep straight tangent, and (3) the maximum load at large displacement.

For lateral pipeline/soil interaction events (Fig. 3), there is a clear differences in soil failure development around the pipeline as a function of pipeline burial depth ratio (Fig. 3): at shallower depth (H/D = 1.8) it is observed to be the extension of a circular failure surface to the soil surface, which develops the forward upheaval and backward subsidence of the soil surface. For deeper burial depth (H/D = 3.6), a local shear failure mode around the pipe is occurred with a little soil surface variation. This description on soil failure mechanism is consistent with the results from other studies using ABAQUS/Standard (Phillips et al., 2004) and ABAQUS/CEL (Pike and Kenny, 2011) formulations.

Regarding axial pipeline/soil interaction events (Fig. 4), there is found to be an annular shearing zone around the pipe during relative axial soil movement, which is mobilized by the adhesion factor at pipeline-soil interface. This finding is similar to the results from full-scale tests and corresponding 2D FE simulations (Wijewickreme et al., 2009).

From the results of lateral pipeline/soil interaction with H/D = 1.8 (Fig. 5), it can be stated that there is good agreement between the lateral bearing capacity factor of 5.61 using method (3) in this study with the capacity factor of 5.65 by Phillips et al., (2004). There is greater discrepancy with other recommended values such as ALA (2001) of 5.78, and Honegger and Nyman (PRCI, 2010) of 5.81. For deeper burial depth ratio (H/D = 3.6), with the increase of H/D ratio, lateral soil bearing factor is found to fall into an intermediate range between ALA (2001) and PRCI (2004) recommendations.

In terms of numerical modelling formulation, ABAQUS/Standard 3D and ABAQUS/CEL 2D simulations (Phillips et al., 2004, Pike and Kenny, 2011) is shown to be more conservative than LS-DYNA/ALE 3D simulation, according to the H/D ratio increase. Based on the results of axial pipeline/soil interaction (Fig. 6; Honegger et al., 2010), it is found that the adhesion factor ($\alpha = N_y/\pi$ = 0.219 at H/D = 1.8, α = 0.358 at H/D = 3.6) exists in the zone defined by PRCI (2010) lower and upper bound.

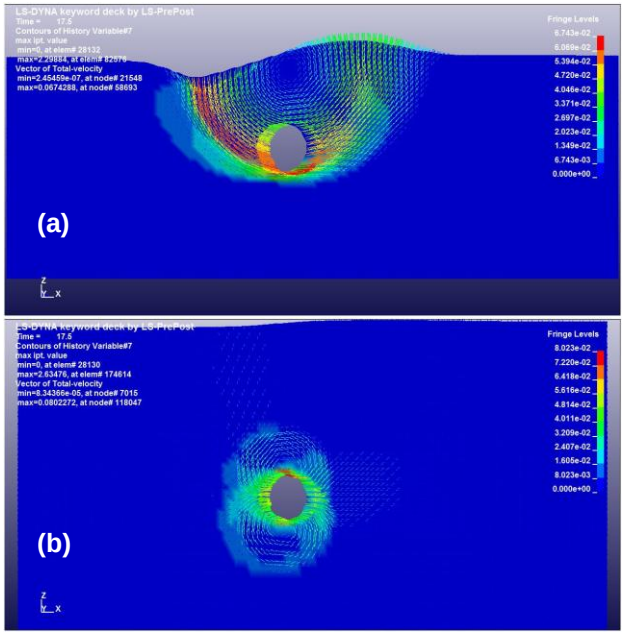

Figure 3. Soil failure mechanisms for lateral pipeline/soil interaction simulations (a) H/D = 1.8, (b) H/D = 3.6

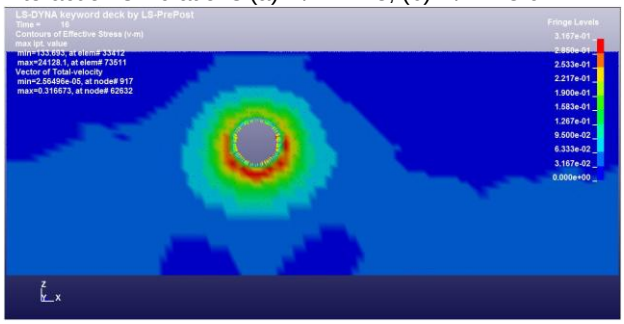

Figure 4. Soil failure mechanism for axial pipeline/soil interaction simulation (H/D = 1.8)

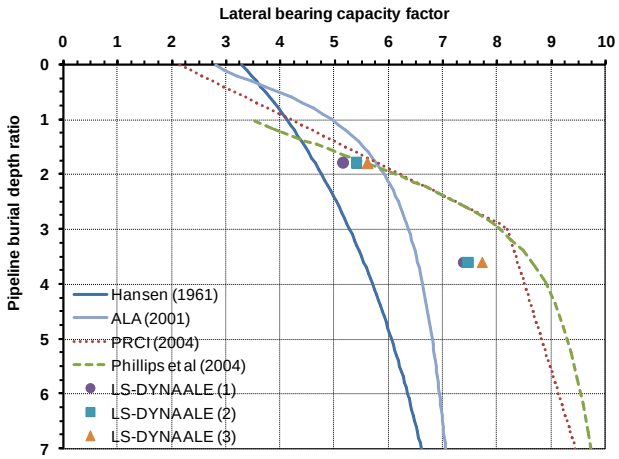

Figure 5. Variation of lateral bearing capacity factor with pipe burial depth ratio

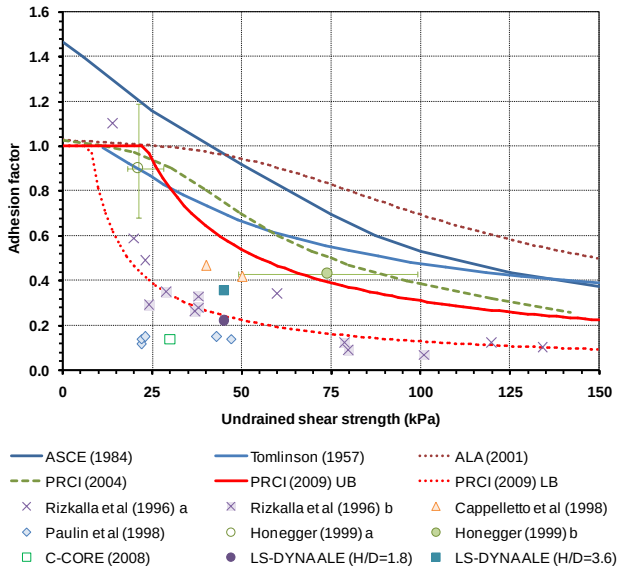

Figure 6. Comparison of axial adhesion factors

4.2 Axial-Lateral Oblique Pipeline/Soil Interaction

Based on the results from oblique pipeline/soil interaction simulations, soil failure mechanisms around the pipe (Fig. 7) was observed as a function of the angle of pipeline oblique movement as follows: As the pipe oblique angle increase, the lateral pipeline/soil interaction force (Fig. 7a, $60^o \le \vartheta \le 90^o$) is manifest in global pipeline/soil behavior, whereas the axial pipeline/soil interaction force (Fig. 7b, $0^o \le \vartheta \le 15^o$) achieve a dominant response mode with a little soil surface heave. Figure 7 also presents a transition zone between two general modes ($15^o \le \vartheta \le 60^o$). As indicated in Fig. 7 and Fig. 8, the maximum axial pipeline/soil interaction force is found around an angle ϑ of 10^o (α = 0.62), which is consistent with the ABAQUS/Standard 3D FE result for clay (Phillips et al., 2004) and different from the centrifuge test data and ABAQUS/Standard 3D FE result for sand ($\vartheta \approx 55^o$, Daiyan et al., 2010). As discussed in Phillips et al., (2004), this study supports that the axial pipeline/soil interaction force is very low for axial pipeline displacement ($\vartheta = 0^o$) irrespective of the pipe burial depth ratio (*H*/*D*).

From these observations, yield envelopes for axial-lateral oblique pipeline/soil interaction can be established as depicted in Fig. 9. For the ultimate load by the method (3), Figure 9 includes the interaction curves proposed by Phillips et al., (2004) and Daiyan et al., (2010):

$$N_x^2 + 3N_y^2 = N_{x90}^2,\ N_y < \alpha\pi \quad for\ clay \qquad [9]$$

$$N_x^2 + N_y^2 = N_{x90}^2 \quad for\ sand \qquad [10]$$

For the range from $\vartheta = 90^o$ to $\vartheta = 15^o$, the yield envelope obtained from this study is found to fall into an intermediate zone between both recommendations. On the same time, Figure 9 suggests that the yield envelope is converging to the α = 0.62 line at the range from $\vartheta = 15^o$ to $\vartheta = 5^o$.

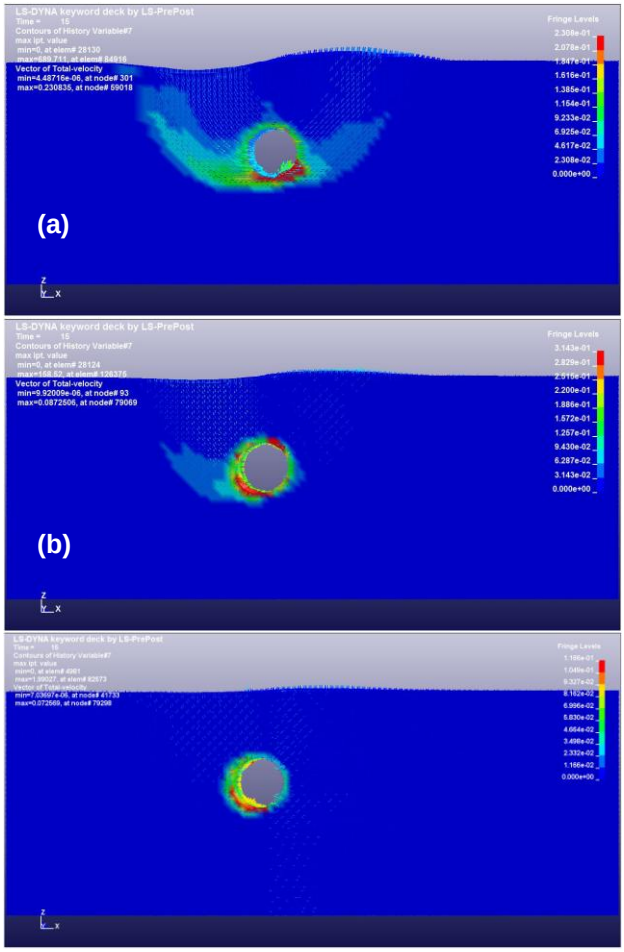

Figure 7. Soil failure mechanisms for axial-lateral oblique pipeline/soil interaction simulations with *H*/*D* = 1.8 (a) $\vartheta = 60^o$, (b) $\vartheta = 30^o$, and (c) $\vartheta = 15^o$

5 CONCLUDING REMARKS

The yield envelopes for axial-lateral oblique pipeline/soil interaction in cohesive soil were investigated with particular attention to the pipe oblique angle and the pipe burial depth ratio on the basis of LS-DYNA/Explicit ALE formulation. Based on the results obtained, the soil failure mechanisms were examined as a function of pipe oblique angle. This paper also presents a fact that the yield envelopes should be determined by considering soil failure mechanisms, which is varied with pipe oblique angle: (a) lateral resistance, (b) lateral-axial transition, and (c) axial resistance resistance zones. In the end, there is a need to conduct further study on the variability of soil/pipe properties, interface properties, contact mechanics, geometric and scaling issues (e.g. pipe diameter and pipe burial depth ratio), soil constitutive models, soil variability and trench effects, and soil strain localization.

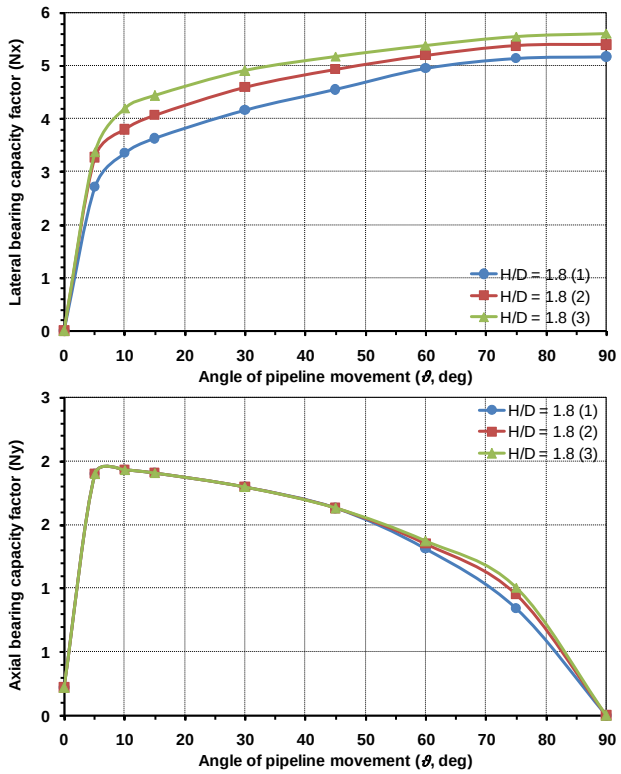

Figure 8. LS-DYNA/ALE FE results: *H*/*D* = 1.8

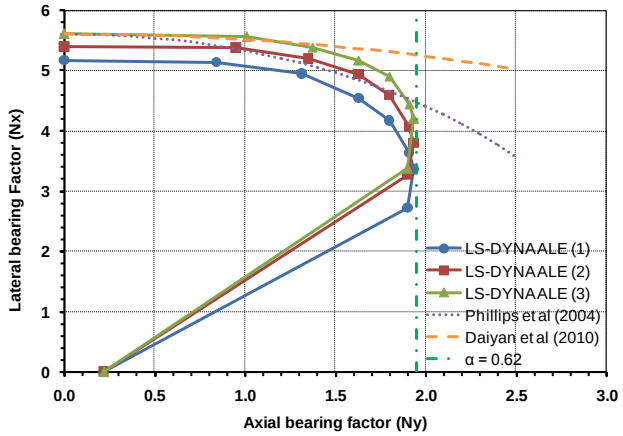

Figure 9. Yield envelopes for axial-lateral oblique pipeline/soil interaction (*H*/*D* = 1.8)

ACKNOWLEDGEMENTS

The writers would like to gratefully acknowledge program funding through MITACS.

REFERENCES

ALA 2001. Guidelines for the Design of Buried Steel Pipe, American Lifelines Alliance.

Banneyake, R., Hossain, M.K., Eltaher, A., Nguyen, T., and Jukes, P. 2011. Ice-soil-pipeline interactions using coupled Eulerian-Lagrangian (CEL) ice gouge simulations - Extracts from Ice Pipe JIP, *Arctic Technology Conf.*, Houston, TX, USA.

Bruschi, R., Bughi, S., and Spinazzè, M. 2010. The role of FEM in the operation of pipelines in unstable soils, *J. of Pipeline Eng.*, 9(3): 167-177.

Cocchetti, G., Prisco, C., Galli, A., and Nova, R. 2009. Soil-pipeline interaction along unstable slopes: a coupled three-dimensional approach. Part 1: Theoretical formulation, *Can. Geotech. J.*, 46:1289-1304.

Daiyan, N., Kenny, S., Phillips, R., and Popescu, R. 2009. Parametric study of lateral-vertical pipeline/soil interaction in clay, *1st Int./1st Eng. Mechanics and Materials Specialty Conf.*, St. John's, NL, Canada.

Daiyan, N., Kenny, S., Phillips, R., and Popescu, R. 2010. Numerical investigation of oblique pipeline/soil interaction in sand, *8th Int. Pipeline Conf.*, Calgary, Alberta, Canada.

Donea, J., A. Huerta, J.-Ph. Ponthot and A. Rodrıguez-Ferran, 2004. Arbitrary Lagrangian–Eulerian methods. *Encyclopaedia of Computational Mechanics*, Erwin Stein, René de Borst and Thomas J.R. Hughes Editors. Volume 1: Fundamentals. John Wiley & Sons.

Fredj, A., Dinovitzer, A., and Zhou, J. 2008. A 3-Dimensional continuum ALE model for soil-pipe interaction, *7th Int. Pipeline Conf.*, Calgary, Alberta, Canada.

Fredj, A. and Dinovitzer, A. 2010. Three-dimensional response of buried pipeline subjected to large soil deformation effects- Part I: 3D continuum modeling using ALE and SPH formulations, *8th Int. Pipeline Conf.*, Calgary, Alberta, Canada.

Guo, P. 2005. Numerical modeling of pipe-soil interaction under oblique loading. *J. of Geotech. and Geoenviron. Eng.*, ASCE, 131(2): 260-268.

Hansen, J.B. 1961. The ultimate resistance of rigid piles against transversal forces, Bulletin 12, Danish Geotechnical Institute, Copenhagen, Denmark.

Honegger, D.G. and Nyman, D.J. 2004. Seismic design and assessment of natural gas and liquid hydrocarbon pipelines, Pipeline Research Council International Project PR-268-9823.

Honegger, D., Popelar, C., Hart, J.D., Phillips R., and Gailing, R. 2010. Recent PRCI guidelines for pipelines exposed to landslide and subsidence hazards, *8th Int. Pipeline Conf.*, Calgary, Alberta, Canada.

Hsu, T.-W., Chen, Y.-J., and Hung, W.-C. 2006. Soil restraint to oblique movement of buried pipes in dense sand, *J. of Transp. Eng.*, ASCE, 132(2): 175-181.

Jukes, P., Eltaher, A., Abdalla, B., and Duron, B. 2008. The design and simulation of arctic subsea pipelines, DNV Conf. on Arctic Activities, Høvik.

Kenny, S., Barrett, J., Phillips, R., and Popescu, R. 2007a. Integrating geohazard demand and structural capacity modelling within a probabilistic design framework for offshore arctic pipelines, *17th Int. Offshore and Polar Eng. Conf.*, ISOPE, Lisbon, Portugal.

Konuk, I. and Gracie, R. 2004. A 3-Dimensional Eulerian finite element model for ice scour, *5th Int. Pipeline Conf.*, Calgary, Alberta, Canada.

Konuk, I., Yu, S., and Fredj, A. 2006. Do Winkler models work: A case study for ice scour problem, *25th Int. Conf. on Offshore Mechanics and Arctic Eng.*, Hamburg, Germany.

Konuk, I. and Yu, S. 2007. A pipeline case study for ice scour design, *26th Int. Conf. on Offshore Mechanics and Arctic Eng.*, San Diego, California, USA.

Konuk, I. and Yu, S. 2007. Continuum FE modeling of lateral buckling: Study of soil effects, *26th Int. Conf. on Offshore Mechanics and Arctic Eng.*, San Diego, California, USA.

Lele, S.P., Hamilton, J.M., Panico, M., Arslan, H., and Minnaar, K. 2010. 3D Continuum simulation to determine pipeline strain demand due to ice-gouge hazards, *Arctic Technology Conf.*, Houston, TX, USA.

LSTC 2006. LS-DYNA Theory manual, LSTC, Livermore, CA, USA.

LSTC 2010. LS-DYNA Keyword user's manual, Ver. 971 / Rev. 5, LSTC, Livermore, CA, USA.

Phillips, R., Barrett, J., and Al-Showaiter, A. 2010. Ice keel-seabed interaction: Numerical modeling validation, *Offshore Technology Conf.*, Houston, TX, USA.

Phillips, R., Nobahar, A., and Zhou, J. 2004. Combined axial and lateral pipe-soil interaction relationship, *5th Int. Pipeline Conf.*, Calgary, Alberta, Canada.

Phillips, R., Nobahar, A., and Zhou, J. 2004. Trench effects on pipe-soil interaction, *5th Int. Pipeline Conf.*, Calgary, Alberta, Canada.

Pike, K. and Kenny, S. 2011. Advancement of CEL procedures to analyze large deformation pipeline/soil interaction events, *Offshore Technology Conf.*, Houston, TX, USA.

Pike, K., Seo, D., and Kenny, S. 2011. Continuum modelling of ice gouge events: Observations and assessment, *Arctic Technology Conf.*, Houston, TX, USA.

Wijewickreme, D., Karimian, H., and Honegger, D. 2009. Response of buried steel pipelines subjected to relative axial soil movement, *Can. Geotech. J.*, 46:735-752.

Yimsiri, S., Soga, K., Yoshizaki, K., Dasari, G.R., and O'Rourke, T.D. 2004. Lateral and upward soil-pipeline interactions in sand for deep embedment conditions, *J. of Geotech. and Geoenviron. Eng.*, ASEC, 130(8): 830-842.